Effect of Ni(II) doping on the structure of L-histidine hydrochloride monohydrate crystals

2008 J. Phys.: Condens. Matter 20 275209

(http://iopscience.iop.org/0953-8984/20/27/275209)

J. Phys.: Condens. Matter **20** (2008) 275209 (6pp) doi:10.1088/0953-8984/20/27/275209

Effect of Ni(II) doping on the structure of L-histidine hydrochloride monohydrate crystals

C M R Remédios[1], W Paraguassu[2], J A Lima Jr[3], P T C Freire[3], J Mendes-Filho[3], F E A Melo[3], A S de Menezes[4], A O dos Santos[4], L P Cardoso[4] and M A R Miranda[5,6]

[1] Universidade Federal do Pará Campus de Santarém, 68040-070, Santarém, PA, Brazil
[2] Departamento de Física, Universidade Federal do Maranhão, 65085-580, São Luiz, MA, Brazil
[3] Departamento de Física, Universidade Federal do Ceará, PO Box 6030, 60455-900, Fortaleza, CE, Brazil
[4] DFA, IFGW, UNICAMP, CP 6165, 13083-970 Campinas, SP, Brazil
[5] Department of Physics, University of Guelph, N1G 2W1l, Guelph, ON, Canada

E-mail: marcus@physics.uoguelph.ca

Received 23 March 2008, in final form 7 May 2008
Published 3 June 2008
Online at stacks.iop.org/JPhysCM/20/275209

Abstract

In this paper, we study the effect of Ni(II) doping on the structure of L-histidine hydrochloride monohydrate crystals using x-ray diffraction and Raman spectroscopy. X-ray powder diffraction shows no significant change in the unit cell parameters of the doped single crystal, whereas x-ray multiple diffraction using synchrotron radiation indicates that the Ni ions are located in interstitial positions in the crystal lattice. The temperature-dependent Raman spectra reveal a structural phase transition in the 10–300 K temperature range. The proposed mechanism of this phase transition supports the suggestion that the Ni ions occupy interstitial positions.

(Some figures in this article are in colour only in the electronic version)

1. Introduction

The structural stability of amino acid crystals is one of many lines of current research. These materials have several possible technological applications in the pharmaceutical and electronics industries, such as in electro-optical devices and the treatment of allergic diseases and anaemia [1]. L-histidine is one of the protein-forming amino acids, playing a fundamental role in several biological mechanisms, including the formation of haemoglobin. When it is grown in aqueous solution at pH 7, L-histidine crystallizes with water molecules inside the structure, forming an L-histidine hydrochloride monohydrate crystal, $C_6H_{10}N_3O_2{\cdot}HCl{\cdot}H_2O$ (LHICL). This crystal has four molecules per unit cell, belongs to the orthorhombic system (space group $P2_12_12_1$) and its lattice parameters are $a = 15.301(3)$ Å, $b = 8.921(2)$ Å and $c = 6.846(2)$ Å [2]. The vibrational and optical properties of amino acid crystals have received much theoretical and experimental attention in recent years. Knowledge of the vibrational structure of LHICL is fundamental for crystal engineering and for the design of supramolecular devices. In a previous work, single crystals of LHICL were studied by Raman spectroscopy [3]. The behaviour of its vibrational spectrum indicates that this material undergoes a structural phase transition below 140 K and perhaps a second phase transition between 80 and 60 K.

In recent years, great attention has been paid to the study of the influence of doping on several crystals, in particular because doping can modify the physical properties of materials for technological applications [4–7]. For example, certain transition metal ions often modify the growth habit of a crystal when incorporated into the lattice. The optimization of size and shape is of fundamental importance in the crystallization industry and growth-modifying additives are often used to control the relative growth rates of the various crystal faces in order to achieve a particular shape.

[6] Author to whom any correspondence should be addressed.

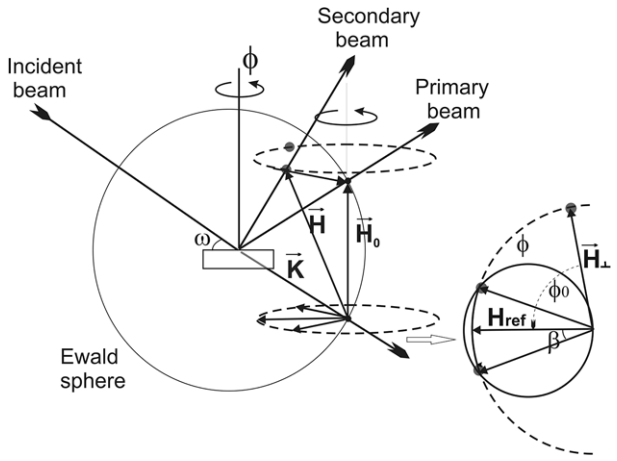

Figure 1. Reciprocal lattice representation of multiple diffraction.

X-ray diffraction techniques are normally preferred for analysing structural changes in crystal lattices since they probe atomic positions directly and provide important information not available when other techniques are used. In particular, x-ray multiple diffraction has been applied as a high resolution probe to investigate subtle changes in single crystal lattices, for example, in the application of an external electric field to single crystals in order to determine the piezoelectric coefficients [8, 9], in ion implanted semiconductors to study the interstitial rich and the matrix regions in shallow junctions [10] and in trivalent Mn ion doped KDP crystals to study habit modification [4]. Since it is not a conventional technique, we will give a brief description in the next paragraph.

The multiple diffraction phenomenon arises when an incident beam simultaneously satisfies Bragg's law for more than one set of lattice planes within the crystal. To obtain x-ray multiple diffraction, the primary plane is adjusted to diffract the incident beam. With the rotation (ϕ angle) of the sample around the primary reciprocal lattice vector ($\mathbf{H}_0$), several other planes called secondary and coupling, will also enter into the diffraction conditions simultaneously with the primary. These coupling planes establish the interaction between the primary and the secondary beams. In the pattern I_{primary} versus ϕ, called a Renninger scan [11], positive and negative peaks are distributed according to the symmetry of the primary vector and the symmetry plane established by the ϕ rotation. The peak position in a Renninger scan is given by $\phi = \phi_o \mp \beta$ where ϕ_o is the angle between $\mathbf{H}_\perp$ (the component of $\mathbf{H}$ on a plane perpendicular to $\mathbf{H}_0$) and $\mathbf{H}_{\text{ref}}$, the reference vector, and 2β is the angle between the entrance and the exit of $\mathbf{H}_\perp$ on the Ewald sphere, as shown in figure 1.

In this work, Ni doping does not change the symmetry or the unit cell parameters of LHICL. However, it does change some features in the peak profiles of the Renninger scan. Based on these changes we propose that the Ni ions are located in interstitial positions in the lattice. Another effect of Ni doping is the appearance of a structural phase transition in the 10–300 K temperature range. This transition can be explained by the presence of Ni on the interstices of the lattice.

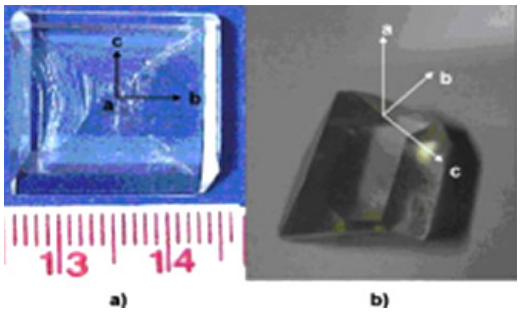

Figure 2. Single crystal photographs: (a) pure and (b) Ni-doped L-histidine hydrochloride monohydrate crystals.

2. Experimental details

LHICL single crystals were grown by slow evaporation of a supersaturated aqueous solution containing L-histidine powder at a controlled temperature of 313 K. Ni-doped LHICL single crystals were prepared in the same manner with the addition of $NiCl_2{\cdot}6H_2O$. An Ni content of 5% (weight) was measured by x-ray fluorescence. Figures 2(a) and (b) show pure and Ni(II)-doped single crystals, respectively.

X-ray powder diffraction was carried out on a Philips X'Pert MRD diffractometer operating at 40 kV/40 mA using Cu Kα radiation and a pyrolytic graphite diffracted beam monochromator. The diffraction patterns were obtained in the angular range of 10°–55° (2θ) with a step size of 0.02° (2θ) and a counting time of 12 s/step. The sample was put to oscillate in order to prevent preferred orientation effects. The diffraction patterns were analysed by Rietveld refinement using the Dbws9807 software [12, 13]. The high resolution Renninger scans were carried out at the XRD1 station in the Brazilian synchrotron radiation facility (LNLS), Campinas, SP, Brazil. The XRD1 station had a Huber three-axis goniometer (ω, φ and 2θ) available with minimum ω and φ axes step sizes of 0.0002° and 0.0005°, respectively. The wavelength used was $\lambda = 1.5387(1)$ Å, determined using a silicon [111] crystal.

The backscattering light was analysed using a Jobin Yvon Triplemate 64000 micro-Raman system equipped with a nitrogen-cooled CCD system. The excitation source for the Raman experiment was 514.5 nm radiation from an argon ion laser with a 2 cm^{-1} spectral resolution set by the slits. All measurements were performed using a long working distance plano-achromatic objective with $f = 20.5$ mm to avoid the propagation of oblique phonons. For the low temperature Raman measurement, the samples were placed in a closed-cycle helium refrigerator that controlled the temperature with a precision of ±0.1 K.

3. Results and discussion

The Ni doping affected the external morphology of the LHICL crystal. Figure 2 shows that the Ni-doped crystal has a different growth habit and colour. Both x-ray powder diffraction and x-ray multiple diffraction show that pure and doped LHICL crystals have the same symmetry and almost identical unit cell parameters (see table 1, figures 3 and 4). These

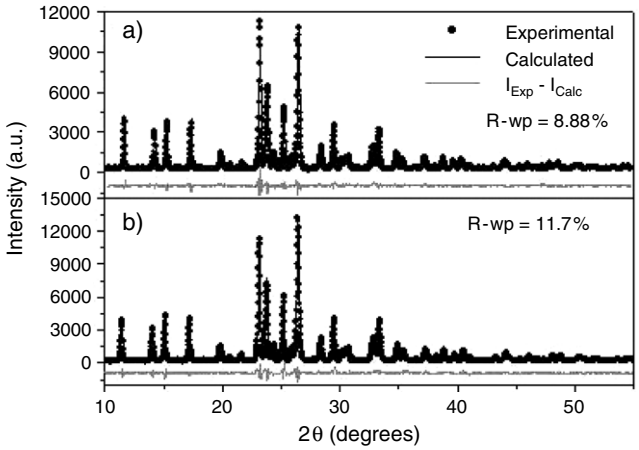

Figure 3. X-ray powder diffraction patterns of (a) pure and (b) doped LHICL. Both patterns are almost identical. This similarity indicates that the symmetry and unit cell of both crystals are almost the same.

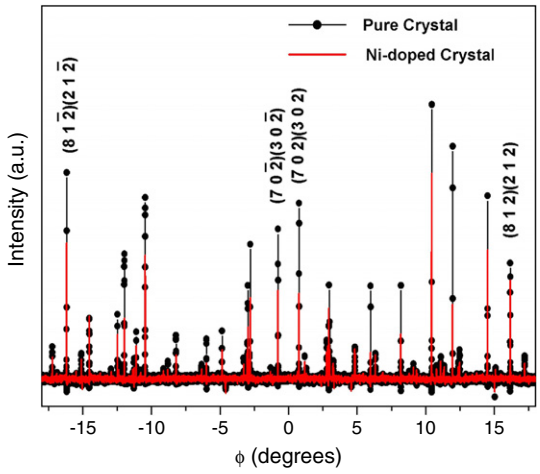

Figure 4. Renninger scans around the $\phi = 0°$ symmetry mirror for the pure and Ni-doped L-histidine hydrochloride monohydrate crystals, using the (10 0 0) as the primary reflection. Both scans are almost identical, which indicates that the unit cell parameters and the symmetry are almost the same in both crystals.

x-ray diffraction results mean that the distortions in the atomic structure are subtle and beyond the reach of x-ray powder diffraction or a superficial x-ray multiple diffraction analysis.

A close examination of the peak profiles in a Renninger scan can reveal features at the atomic level related to the crystalline perfection. Figure 5 shows an expanded region of the Renninger scan around $\phi = 21°$. We see two effects of the Ni doping in the LHICL: first, the $(60\bar{4})$ $(\bar{4}0\bar{4})$ four-beam peak intensity practically disappears. This effect can be due to a small change in atomic positions in the unit cell. Second, there is an evident broadening of the $(3\bar{1}\bar{1})$ $(7\bar{1}\bar{1})$ peak that can be associated with a larger mosaic spread in the doped crystal. Third, the $(3\bar{1}\bar{1})(7\bar{1}\bar{1})$ peak loses part of its asymmetric character. Perfect or near perfect crystals, such as the pure LHICL sample, show highly asymmetric peaks in a Renninger scan due to the small loss of coherence of the waves diffracted by different portions of the crystal (dynamical regime). In

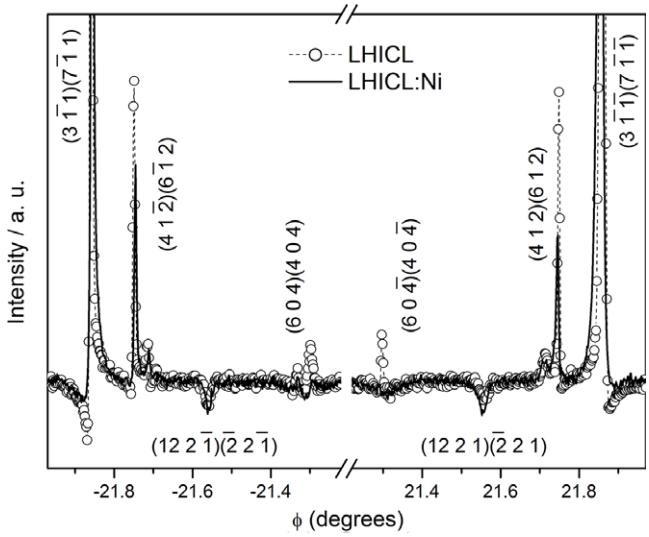

Figure 5. Renninger scans around $\phi = 21.6°$ and $-21.6°$ using (10 0 0) as the primary reflection. In this region, the negative peak corresponding to the $(12\bar{2}\bar{1})(\bar{2}21)$ four-beam case is the most sensitive to detect small variations in the lattice parameters, since its β value (54.6°) is the smallest. We see no variation in its angular position when comparing both samples, which means that lattice parameters are almost identical in both samples. On the other hand, we see the effect of Ni doping on the disappearance of the $(60\bar{4})(\bar{4}0\bar{4})$, the broadening and loss of asymmetry of the $(3\bar{1}\bar{1})(7\bar{1}\bar{1})$.

Table 1. Lattice parameters obtained by Rietveld refinement of x-ray powder diffraction patterns. The R factors were $R_{wp} = 8.88\%$ and $R_{\text{Bragg}} = 4.1\%$ for the pure sample and, $R_{wp} = 11.7\%$ and $R_{\text{Bragg}} = 4.77\%$ for the Ni-doped sample.

Crystal	a (Å)	b (Å)	c (Å)	Volume (Å^3)
Pure LHICL	15.3117(8)	8.9292(5)	6.8515(4)	936.746
Ni-doped LHICL	15.3109(9)	8.9280(6)	6.8509(4)	936.483

this regime, the amplitude of the wave fields from the various portions of the crystal add together, generating the asymmetric peak profile. On the other hand, the peaks in the doped crystal show Gaussian type profiles. These profiles are usually found in crystals with high defect concentration, strain, or high mosaic spread due to great loss of coherence between the waves diffracted by different regions of the crystal (kinematical regime). The diffracted beam consists of the sum of incoherent intensities diffracted by different parts of the crystal, which then produces a symmetric peak profile. We believe that these three effects are caused by the strain produced by the Ni atoms on interstitial positions.

We measured the Raman spectra of the Ni-doped LHICL crystal on cooling in the 300–13 K temperature range. Figure 6 shows the room temperature Raman spectra for three scattering geometries and table 2 presents a tentative assignment. The spectra of the Ni-doped LHICL at 300 K have the same features as those of the LHICL [3]; which confirms that both crystals have the same orthorhombic structure at room temperature. On the other hand, we observe strong modifications in the Raman spectra on cooling, including the appearance and splitting of many modes. This process does occur continuously starting

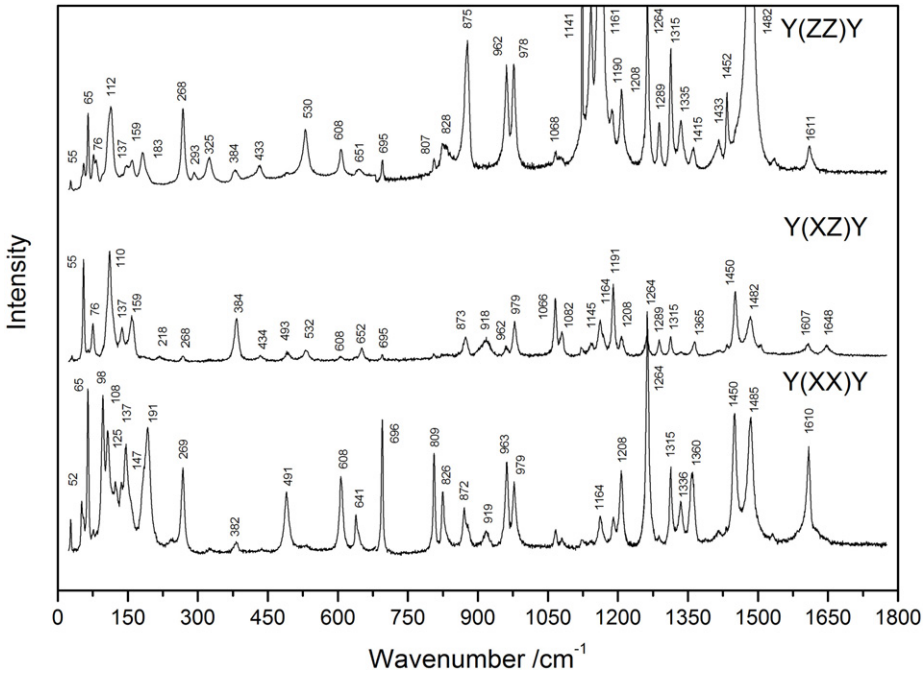

Figure 6. Room temperature Raman spectra of LHICL:Ni recorded in the $y(xx)y$, $y(zx)y$ and $y(zz)y$ scattering geometries in the 1700–35 cm^{-1} region.

Table 2. Vibrational wavenumbers (cm^{-1}) and tentative assignments for the Ni-doped LHICL. (Note: Lat. = lattice; op(CH) = out-of-plane CH deformation; ip(CH)i = in-plane CH deformation of imidazole group; ip(CH)i = in-plane. NH deformation of imidazole; ip(CH)i = in-plane HC deformation of imidazole ring; st. = stretching vibrations of CH, CH_3^+, OH.)

Scattering geometry				Scattering geometry			
$y(xx)y$ (cm^{-1})	$y(xz)y$ (cm^{-1})	$y(zz)y$ (cm^{-1})	Assignment	$y(xx)y$ (cm^{-1})	$y(xz)y$ (cm^{-1})	$y(zz)y$ (cm^{-1})	Assignment
52	55	55	Lat.	919	918		op(CH)
65		65	Lat.	963	962	962	
	76	76	Lat.	979	979	978	
98			Lat.		1066	1068	ip(CH)i
108	110	112	Lat.		1082		
125			Lat.		1145	1141	r(NH_3)
137	137	137	Lat.	1164	1164	1161	ip(NH)i
147			Lat.		1191	1190	
	159	159	Lat.	1208	1208	1208	
		183	Lat.	1264	1264	1264	ip(HC)i
191			Lat.		1289	1289	
	218			1315	1315	1315	
269	268	268		1336		1335	
		293		1360	1365	1363	δ(CH)
		325	δ(struct.)			1415	
382	384	384	τ(NH_3)			1433	
	434	433		1450	1450	1452	
491	493		δ(struct.)	1485	1482	1482	
	532	530	r(CO_2)	1610	1607	1611	ν(C=O)
608	608	608			1648		ν(C=O)
641				2949	2949	2950	st.
	652	651			2973	2973	st.
696	695		δ(CO_2)	3027	3025	3024	st.
809			w(H_2O)	3072	3082		st.
826			γ(CO_2)	3111	3110	3109	st.
872	873	875		3160	3160	3160	st.
				3409	3411	3409	st.

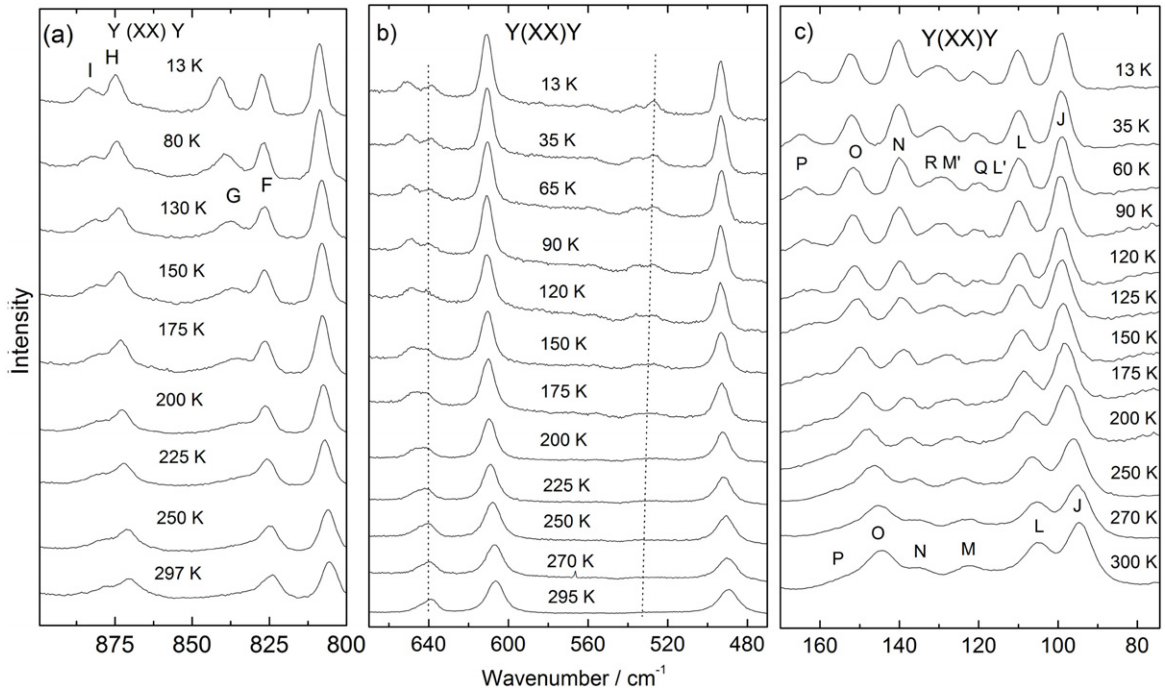

Figure 7. Raman spectra of an LHICL:Ni crystal recorded in the $y(xx)y$ scattering geometry and obtained with decreasing temperature: (a) 900–800 cm^{-1} region, (b) 480–660 cm^{-1} region and (c) 170–75 cm^{-1} region.

from room temperature. Some of these changes are shown in figures 7 and 8 for different frequency ranges and scattering geometries (indicated in the figures in Porto's notation). The following modifications are observed: (1) the appearance of the 115 cm^{-1} (band Q, figure 7(c)), 526 and 533 cm^{-1} (figure 7(b)) and 828 cm^{-1} (figure 7(a)) modes in the $y(xx)y$ scattering geometry; (2) the splitting of the 529 cm^{-1} mode into two modes with frequencies of 527 and 536 cm^{-1} at 13 K (figure 8(a)) in the $y(zz)y$ scattering geometry; (3) the appearance of the 525 cm^{-1} (figure 8(b)), 838, 842, 872 and 943 cm^{-1} modes (figure 8(c)) in the $y(xz)y$ scattering geometry; and (4) in the 80–150 cm^{-1} region of the $y(xx)y$ scattering geometry (figure 7(c)) there are six well-defined bands at room temperature, J, L, M, N, O and P similar to the pure LHICL spectrum. Between bands M and L a new band Q appears and the bands J and L suffer a blue shift as temperature decreases. At 60 K nine bands appear marked in the same spectrum region. Band M splits into bands M′ and R. At room temperature the band N has half the intensity of band O, at 60 K; it has almost double the intensity. Bands P and O suffer blue shifts as temperature decreases.

All these modifications indicate that there is one structural phase transition occurring in the temperature range 300–13 K. These modifications are reversible with temperature. A previously reported [3] phase transition in the pure crystal between 80 and 60 K is not observed in the doped crystal.

Doped and pure samples present basically the same Raman spectrum at room temperature, while on cooling some different features are observed. For the LHICL in the $z(xx)z$ scattering geometry, the 325, 380 and 440 cm^{-1} modes gain intensity and are visible at 40 K (bottom spectra in figure 9). On the other hand, LHICL:Ni exhibits exactly the opposite

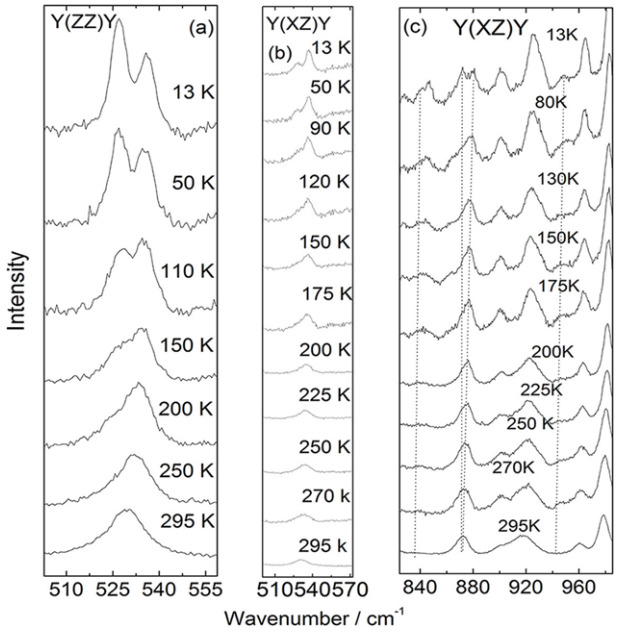

Figure 8. Raman spectra of an LHICL:Ni crystal obtained with decreasing temperature: (a) $y(zz)y$ scattering geometry in the 555–505 cm^{-1} region, (b) $y(xz)y$ scattering geometry in the 510–570 cm^{-1} region and (c) $y(xz)y$ scattering geometry in the 830–970 cm^{-1} region.

behaviour. These modes become weaker on cooling and are almost invisible at 40 K (top spectra in figure 9). These modes are assigned to bending of the structure or rocking of the amino group [3]. One possible explanation for the suppression of these modes is that the Ni ions occupy, in the

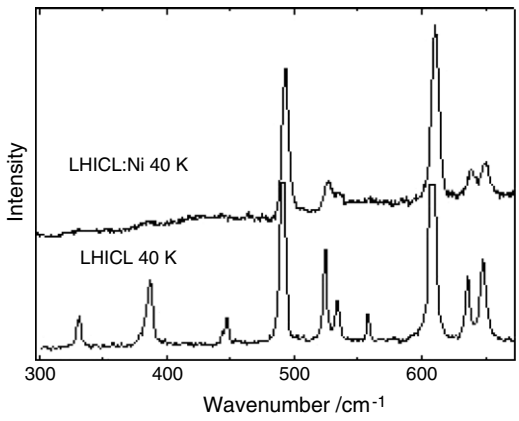

Figure 9. Raman spectra of LHICL and LHICL:Ni at 40 K for $y(xx)y$ scattering geometries in the 300–655 cm^{-1} region.

structure, a position that hinders the low temperature NH_3 rocking motion. Colaneri and Peisach [14] performed an electron spin-echo envelope modulation study on a Cu(II)-doped LHICL system. According to these authors, the copper position is at the midpoint of the amino group of one L-histidine molecule and the imidazole group of another (with Cu(II) . . . N distance of 2.09 Å). We propose in this paper that the Ni ions are located in the same site position that the Cu ions occupy in the LHICL structure, which is reasonable since these ions have similar electronic structures. According to our hypothesis, the interaction between the Ni ions and the NH_3 group increases on cooling due to the packing of the structure so that the rocking motion is progressively hindered and we do not see the area increase (related to mode population) of related Raman modes, as happens in the pure LHICL systems.

4. Conclusion

We studied the structure of pure and Ni-doped LHICL crystals using three techniques: x-ray powder diffraction (Rietveld method) and the x-ray multiple diffraction technique at room temperature, and Raman spectroscopy in the temperature range of 300–13 K. At room temperature, Rietveld analysis showed that the doped sample presented the same structure as the pure one, with a very small change in the lattice parameters. Multiple diffraction results indicated that the Ni ions probably occupy interstitial crystallographic sites in the lattice of the crystal. On cooling we observed one structural phase transition, starting just below room temperature. However, the transition temperature could not be clearly identified. At low temperature the Raman spectra of doped LHICL showed qualitative differences from the pure sample. We proposed in this paper that the Ni ions occupy the same site position as the Cu ions in the LHICL [14] structure. According to our hypothesis, the interaction between the Ni ions and NH_3 group increases on cooling, due to the packing of the structure.

Acknowledgments

We acknowledge the LNLS staff for valuable help during the experiments of multiple diffraction and the financial support from the Brazilian agencies FUNCAP, CNPq and CAPES.

References

[1] Boldyreva E V 2003 *J. Mol. Struct.* **647** 159
[2] Donohue J, Lavine L R and Rollett J S 1956 *Acta Crystallogr.* **9** 655
[3] Faria J L B, Almeida F M, Pilla O, Rossi F, Sasaki J M, Melo F E A, Mendes-Filho J and Freire P T C 2004 *J. Raman Spectrosc.* **35** 242
[4] Lai X, Roberts K J, Avanci L H, Cardoso L P and Sasaki J M 2003 *J. Appl. Crystallogr.* **36** 1230
[5] Cunningham D A H, Hammond R B, Lai X and Roberts K J 1995 *Chem. Mater.* **7** 1690
[6] Lai X, Roberts K J, Bedzyk J M, Lyman P F, Cardoso L P and Sasaki J M 2005 *Chem. Mater.* **17** 4053
[7] Remédios C M R, Paraguassu W, Freire P T C, Mendes-Filho J, Sasaki J M and Melo F E A 2005 *Phys. Rev.* B **72** 014121
[8] Avanci L H, Cardoso L P, Girdwood S E, Pugh D, Sherwood J N and Roberts K J 1998 *Phys. Rev. Lett.* **81** 5426
[9] Avanci L H, Cardoso L P, Sasaki J M, Girdwood S E, Roberts K J, Pugh D and Sherwood J N 2000 *Phys. Rev.* B **61** 6507
[10] Orloski R V, Pudenzi M A A, Hayashi M A, Swart J W and Cardoso L P 2005 *J. Mol. Catal.* A **228** 177
[11] Chang S-L 1984 *Multiple Diffraction of X-rays in Crystals* (Berlin: Springer)
[12] Young R A 1995 *J. Appl. Crystallogr.* **28** 366
[13] Rietveld H M 1967 *Acta Crystallogr.* **22** 151
[14] Colaneri M J and Peisach J 1992 *J. Am. Chem. Soc.* **114** 5335–41